Electronic supplementary information

Ni_2P Immobilized on N,P-Codoped Porous Carbon Sheets for Alkali Metal Ion Batteries and Storage Mechanism

Mingzhe Zhang,[a] Yazhan Liang,[a] Fan Liu,[a] Xuguang An,[b] Jinkui Feng,[c] Baojuan Xi*[a] and Shenglin Xiong*[a]

[a] School of Chemistry and Chemical Engineering, State Key Laboratory of Crystal Materials, Shandong University, Jinan, P.R. China

[b] School of Mechanical Engineering, Chengdu University, Chengdu 610106

[c] School of Materials Science and Engineering, Shandong University, Jinan 250061

*Correspondence author. Email: baojuanxi@sdu.edu.cn (B.J.X.) or chexsl@sdu.edu.cn (S.L.X.)

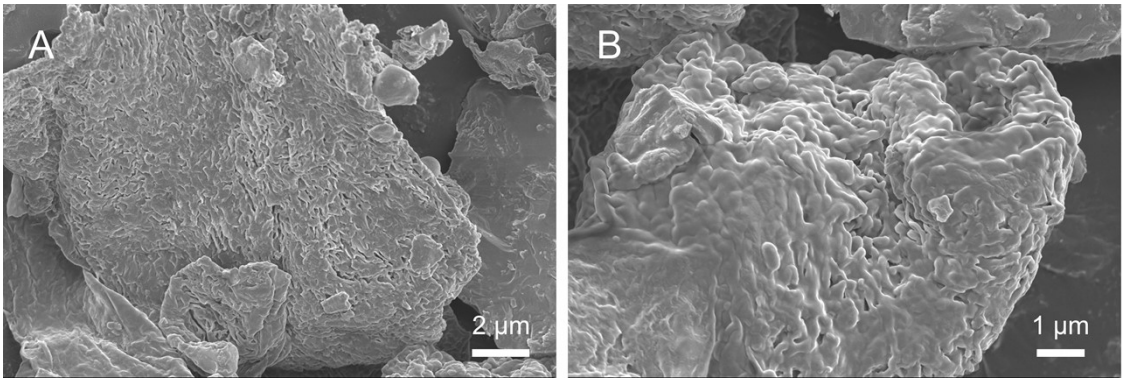

Figure S1. FESEM images of precursor PA-MA-Ni.

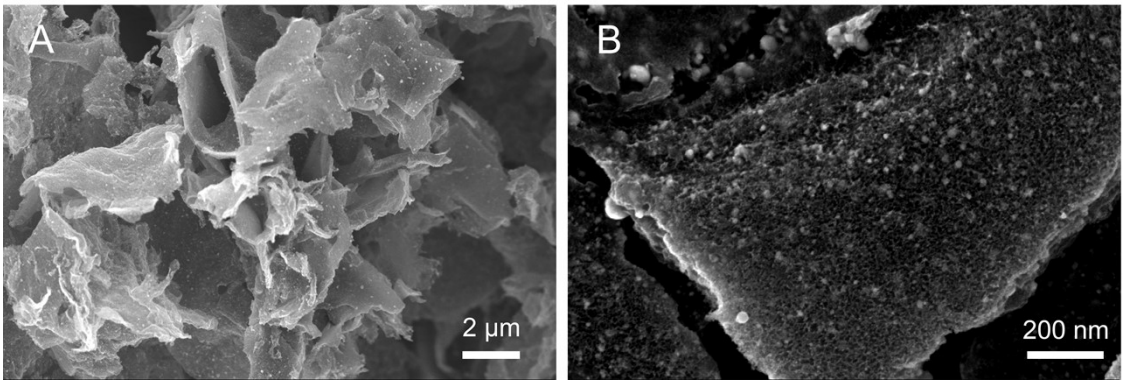

Fig. S2. (A,B) FESEM images of Ni_2P⊂N/P-CNS.

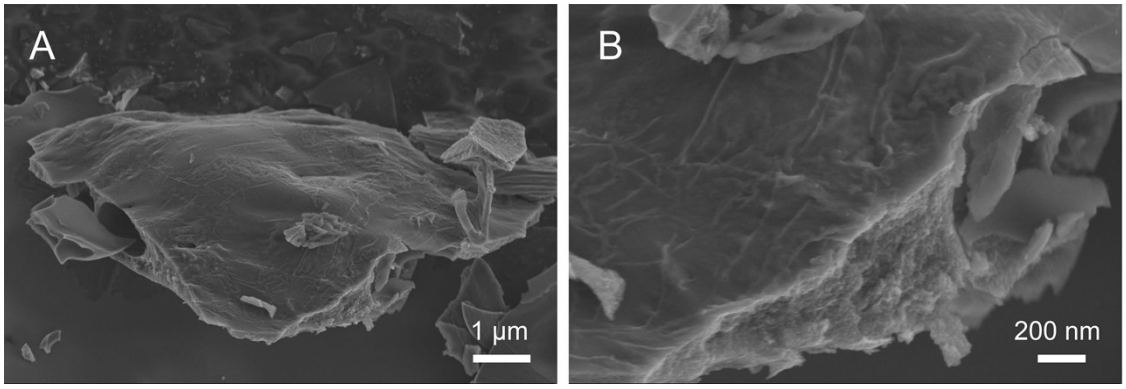

Figure S3. (A,B) FESEM images of N/P-CNS.

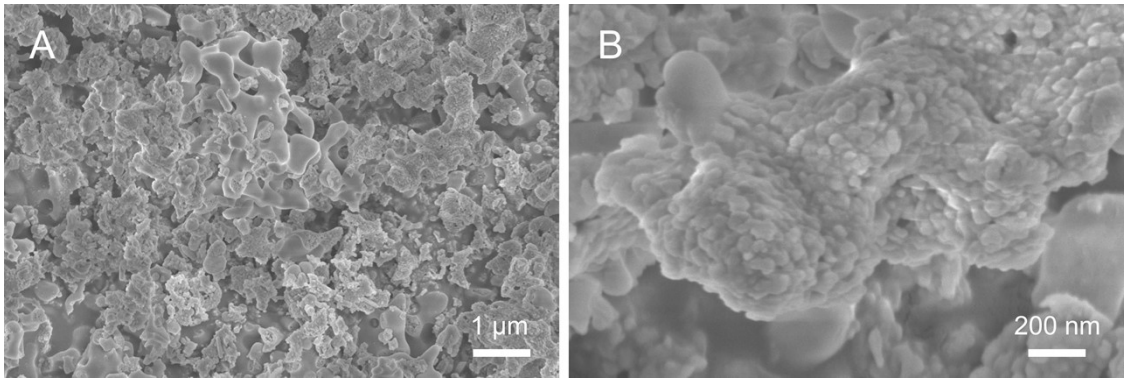

Figure S4. (A,B) FESEM images of Ni_2P.

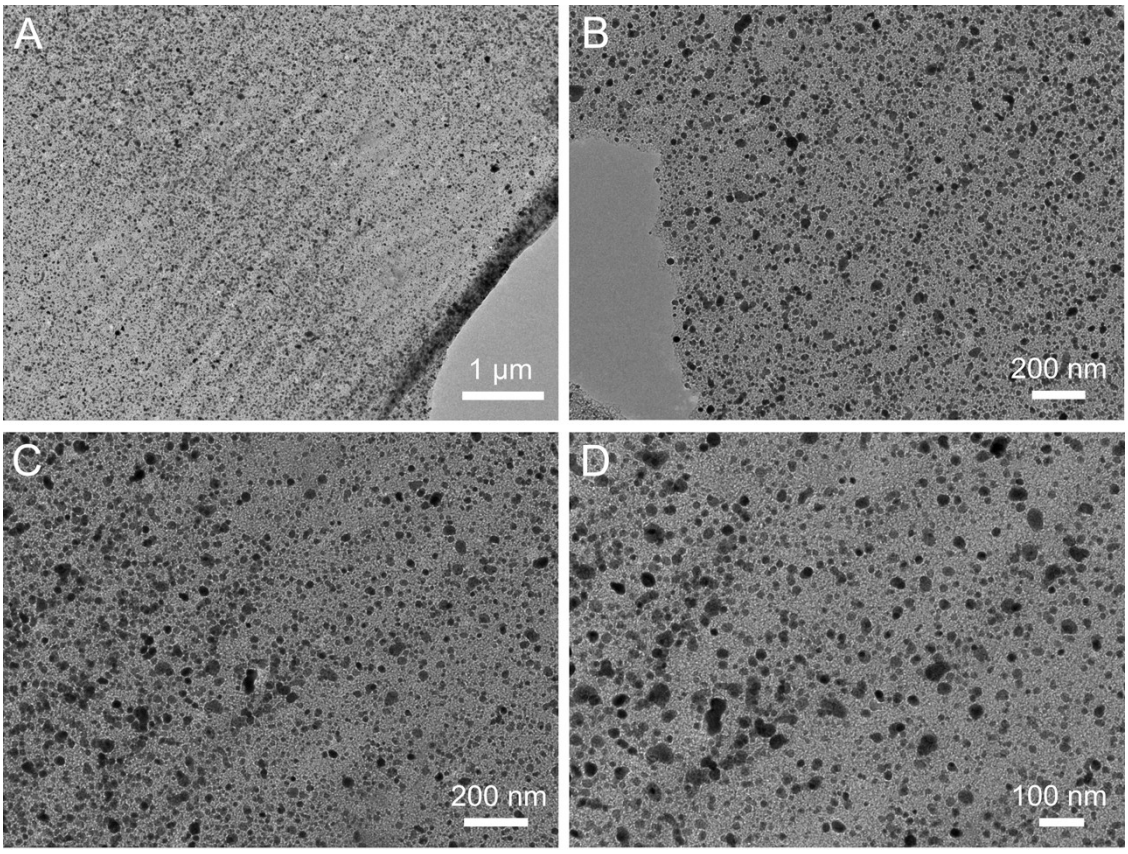

Figure S5. TEM images of Ni_2P⊂N/P-CNS.

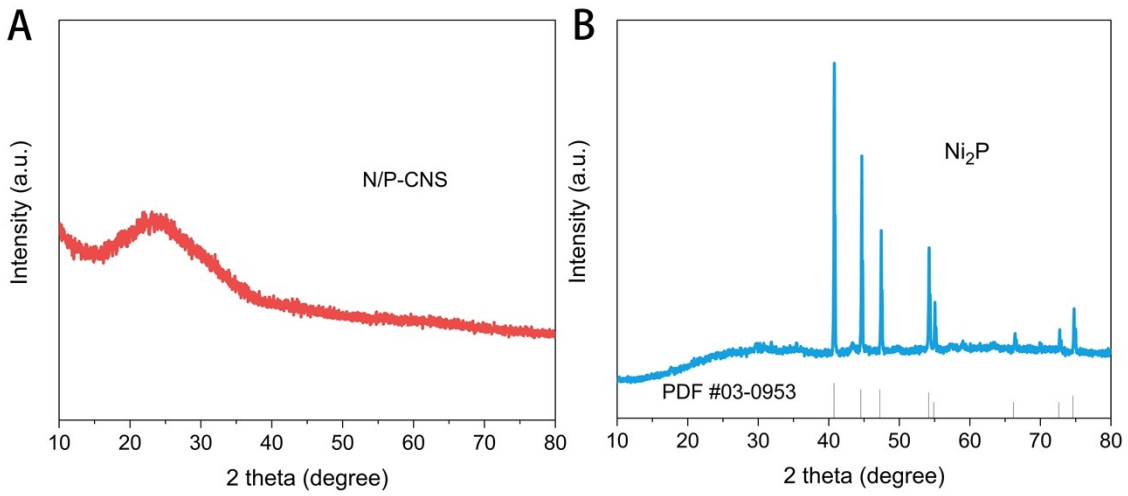

Figure S6. XRD patterns of A) N/P-CNS and B) Ni_2P.

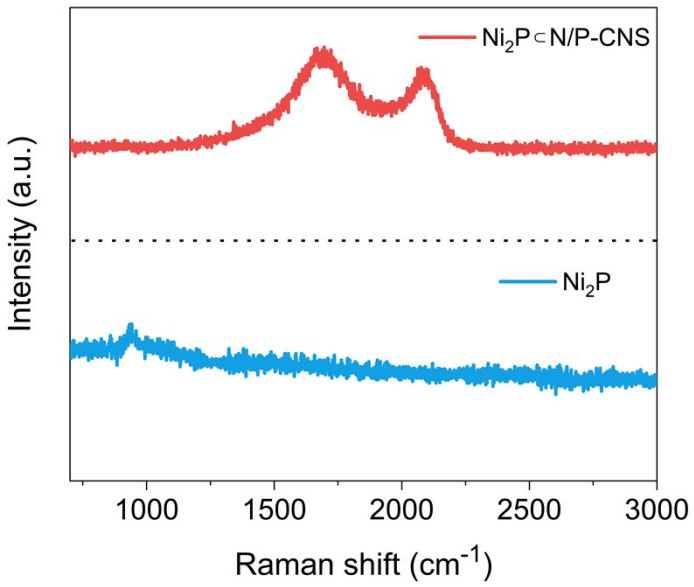

Figure S7. Raman spectra for Ni_2P⊂N/P-CNS and Ni_2P.

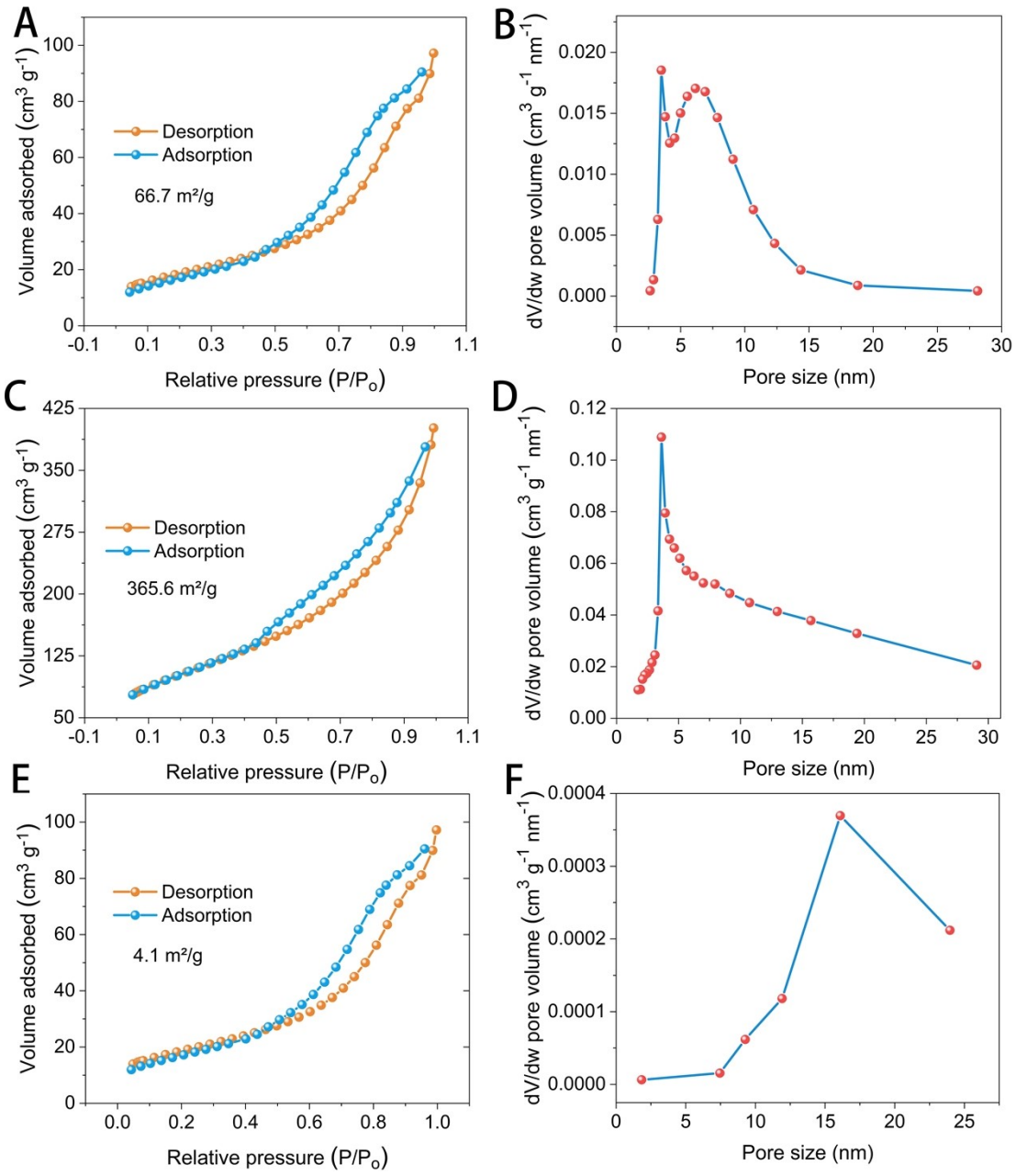

Figure S8. A), C), E) N_2 adsorption-desorption isotherms of the N/P-CNS, Ni_2P⊂N/P-CNS and Ni_2P at 77 K. B), D), F) corresponding pore size distribution.

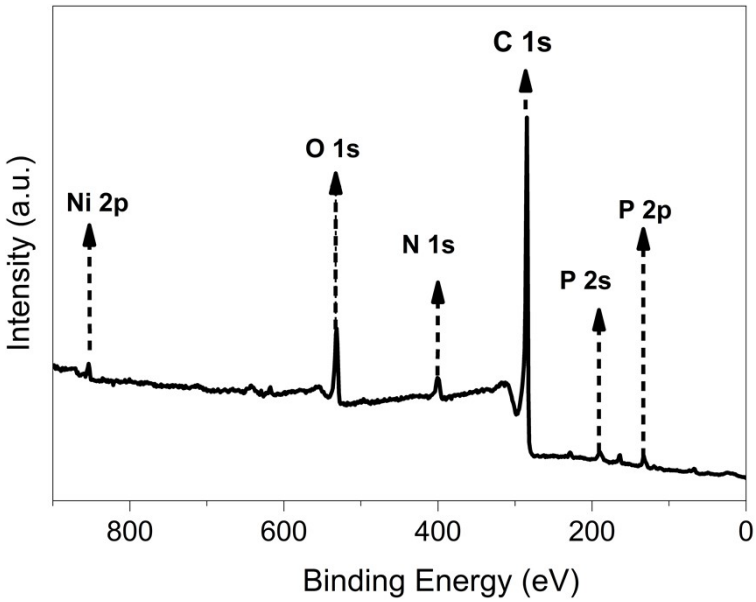

Figure S9. XPS spectrum of Ni_2P⊂N/P-CNS.

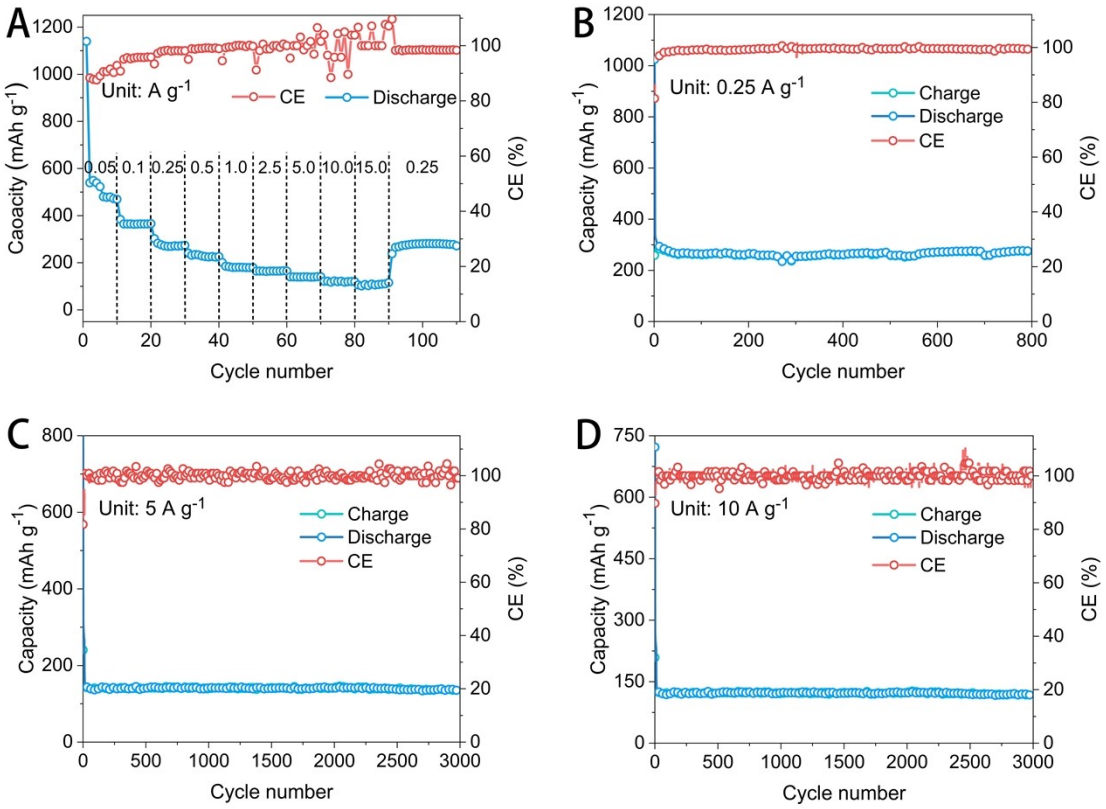

Figure S10. A) Rate performance at different current densities of Ni_2P⊂N/P-CNS and corresponding CE. B−D) Cycling performance and the corresponding CE of Ni_2P⊂N/P-CNS electrodes at 0.25, 5, and 10 A g^{-1}, respectively.

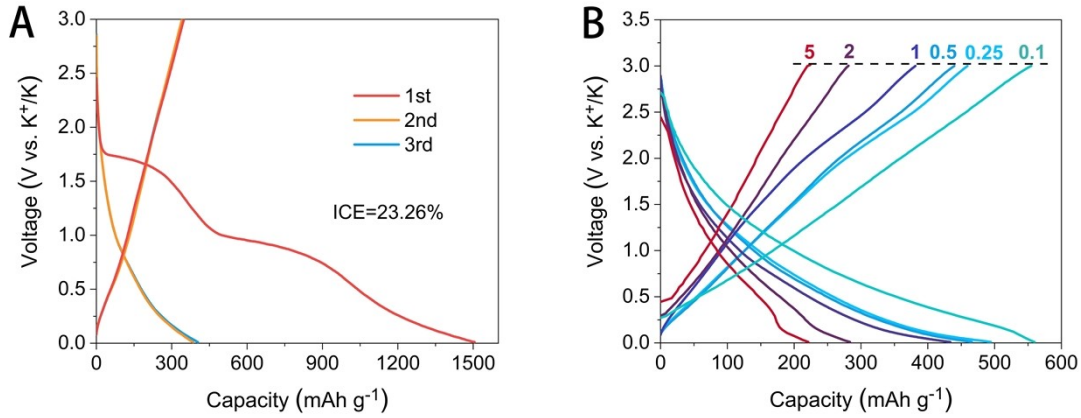

Figure S11. Charge–discharge voltage profiles of A) the first three cycles at a current density of 100 mA g^{-1} and B) at different current densities of Ni_2P⊂N/P-CNS.

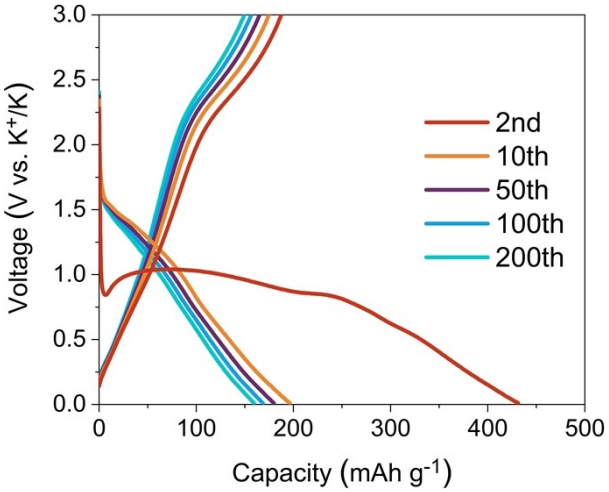

Figure S12. Charge-discharge voltage profiles of Ni_2P at the first five cycles at a current density of 0.1 A g^{-1}.

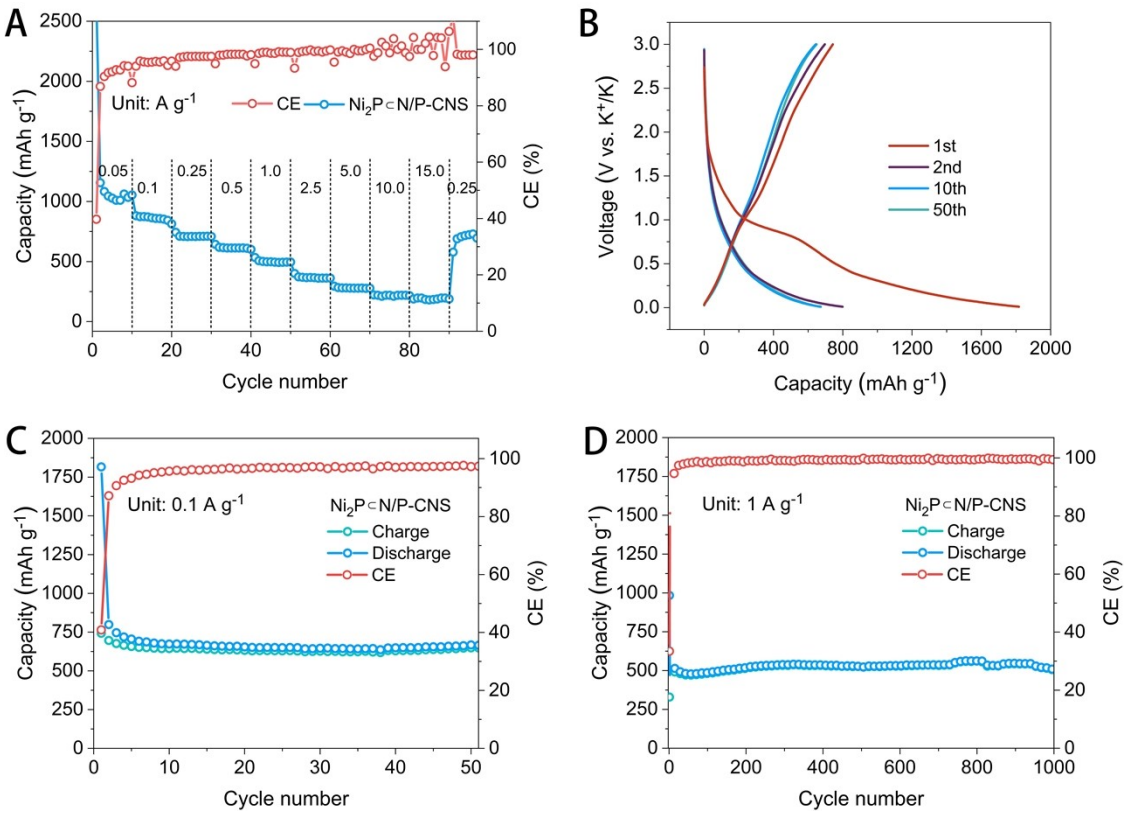

Figure S13. Performance of Ni_2P⊂N/P-CNS as LIB anode material: A) Rate performance at different current densities. B) Charge–discharge voltage profiles at 0.1 A g^{-1}. C,D) Cycling performance and the corresponding CE at 0.1 and 1 A g^{-1}.

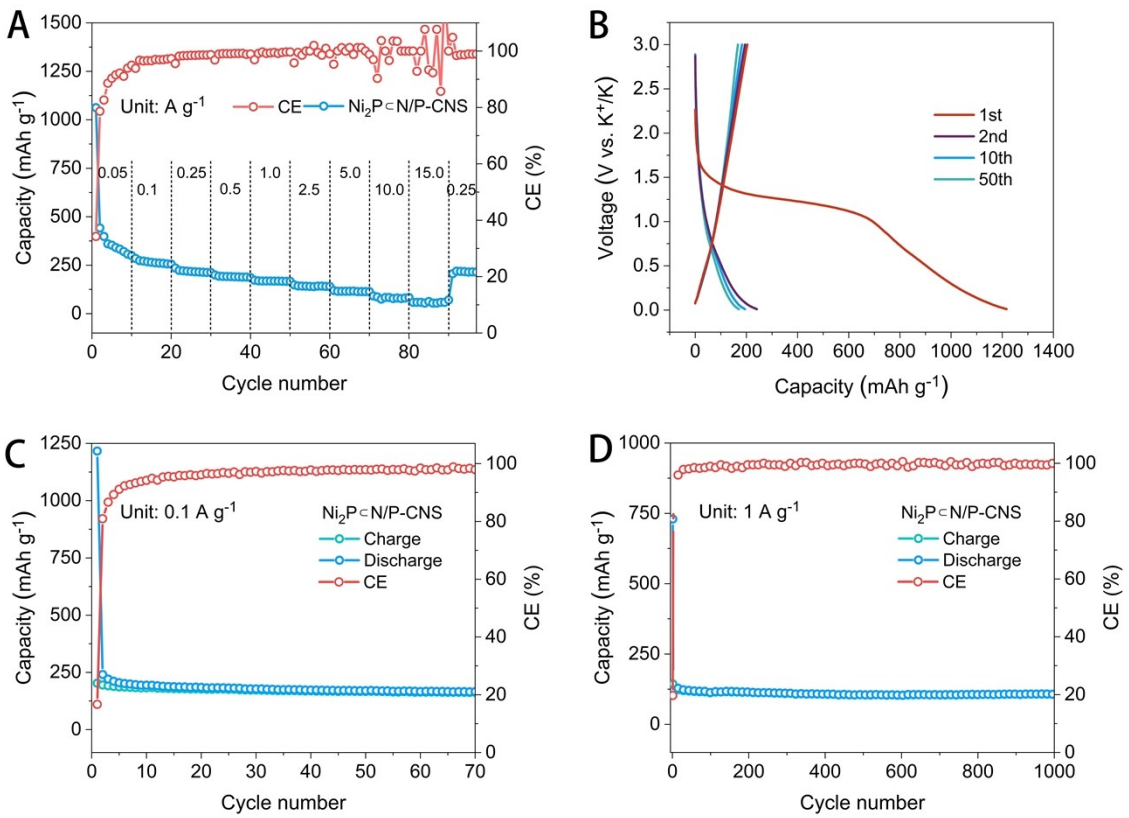

Figure S14. Performance of Ni_2P⊂N/P-CNS as SIB anode material: A) Rate performance at different current densities. B) Charge–discharge voltage profiles at 0.1 A g^{-1}. C,D) Cycling performance and the corresponding CE at 0.1 and 1 A g^{-1}.

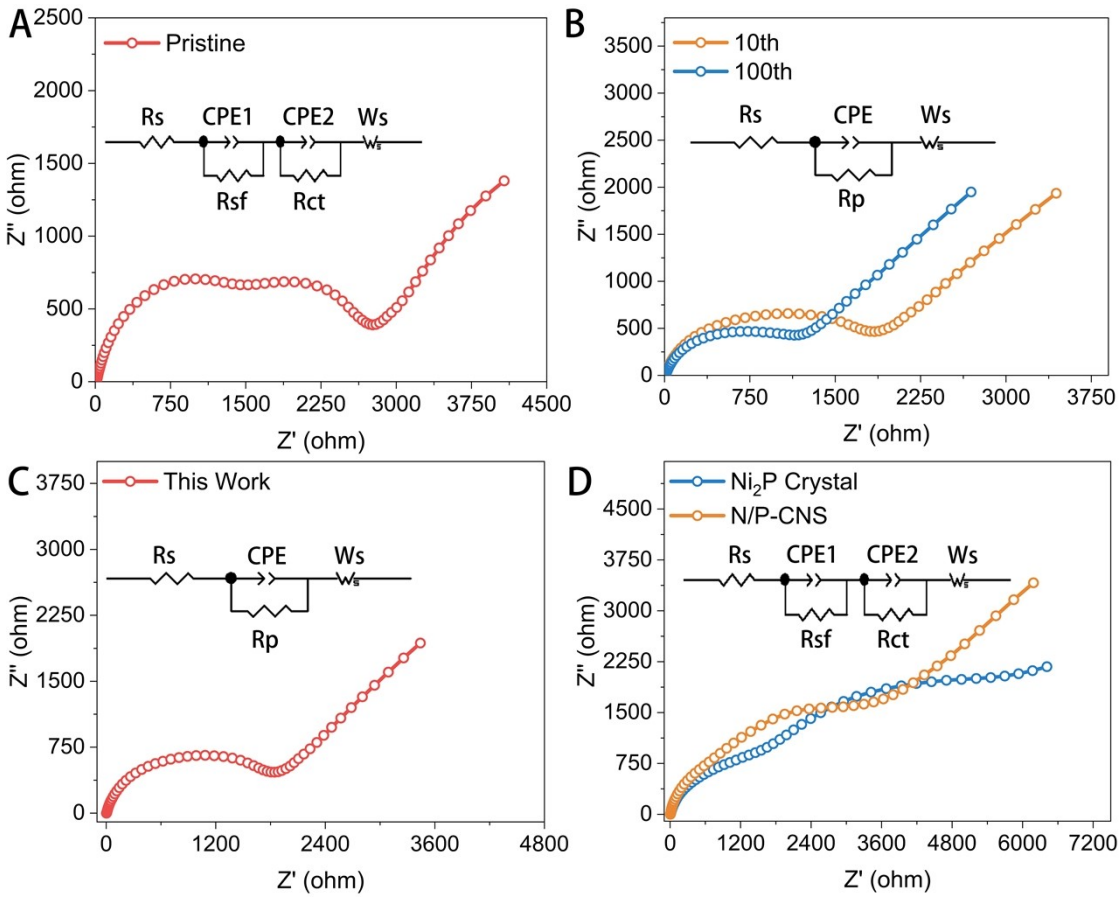

Figure S15. A) Nyquist plots of Ni_2P⊂N/P-CNS at pristine state and B) at 10^{th} and 100^{th} cycle. C) Nyquist plots after initial several cycles of Ni_2P⊂N/P-CNS and D) Ni Crystal and N/P-CNS.

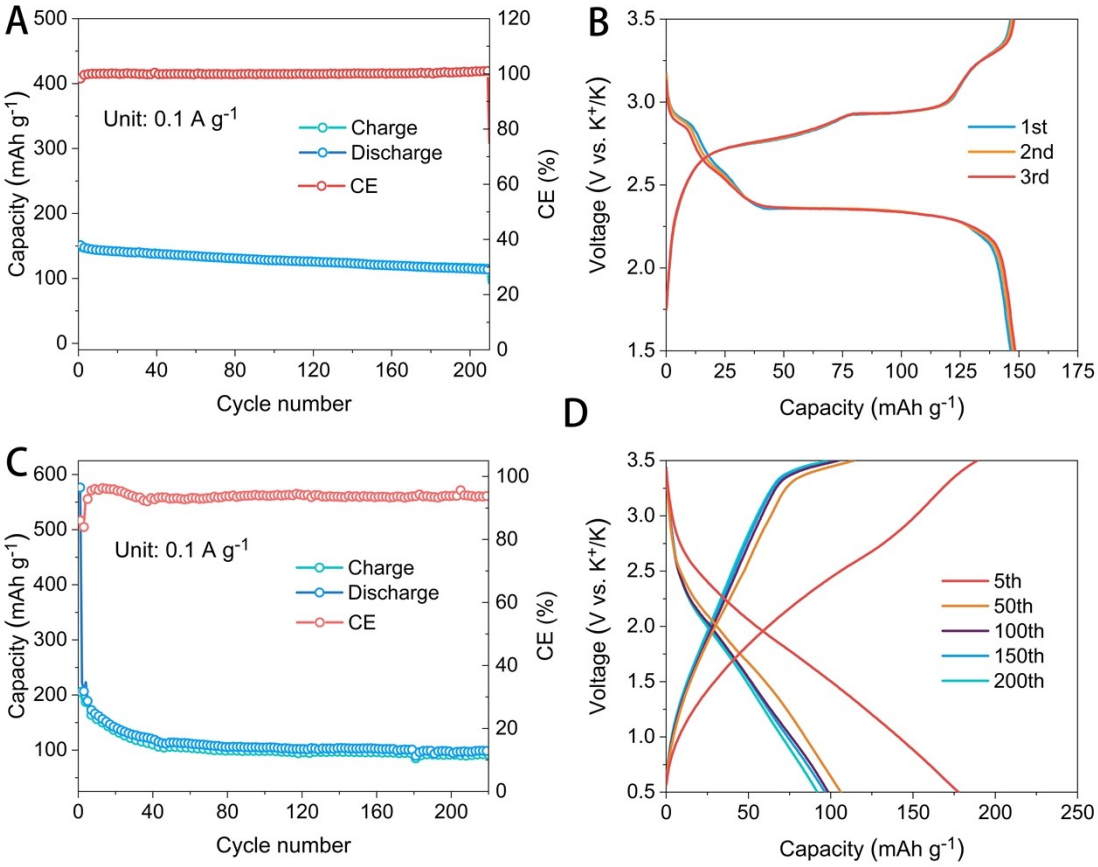

Figure S16. Electrochemical potassium storage performance of the Ni_2P⊂N/P-CNSs //PTCDA K-ion full cell and Ni_2P@NC⊂NCFs anode at high areal loading. A) Cycling performance of the PTCDA cathode at 100 mA g^{-1}. B) Charge–discharge voltage profiles of PTCDA cathode for the initial three cycles at 100 mA g^{-1}. C, D) Cycling performance and charge–discharge voltage profiles of the full cell at 100 mA g^{-1}.

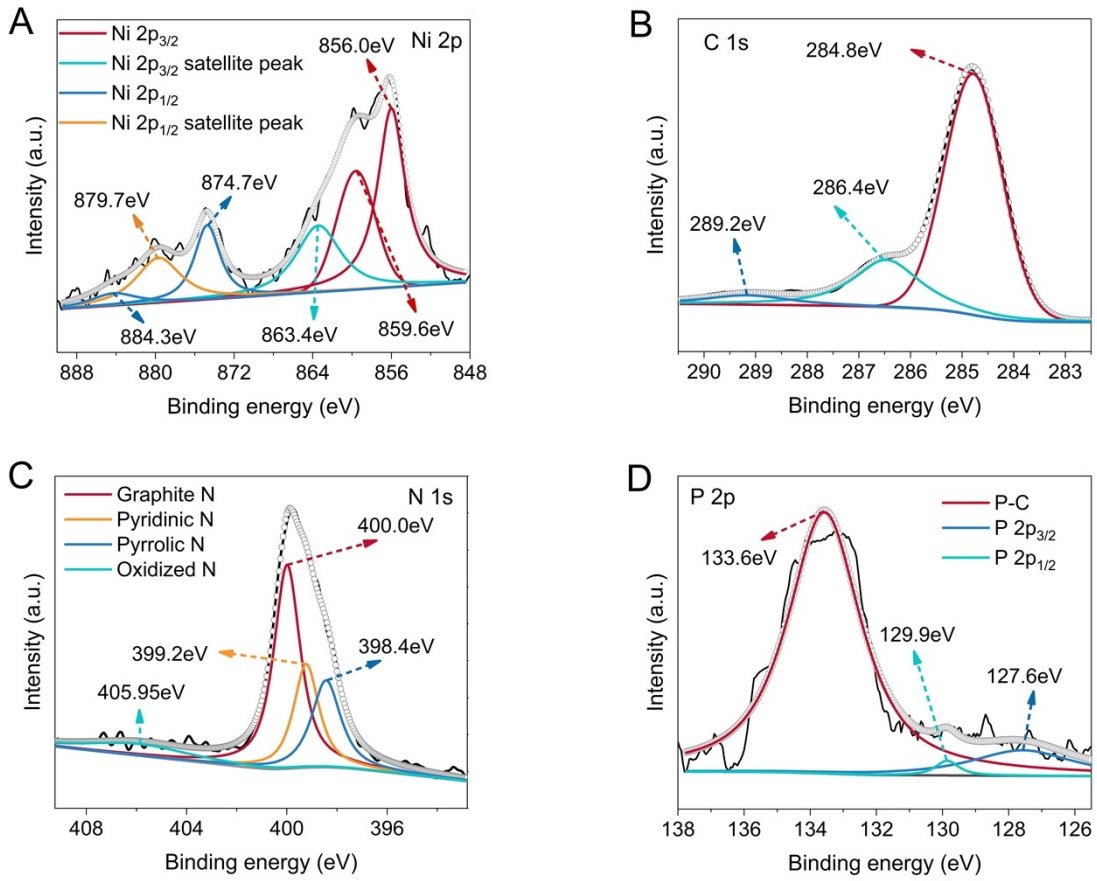

Figure S17. High-resolution XPS spectra of Ni 2p, C 1s, N 1s and P 2p of Ni_2P⊂N/P-CNS electrode after cycling for 100 cycles.

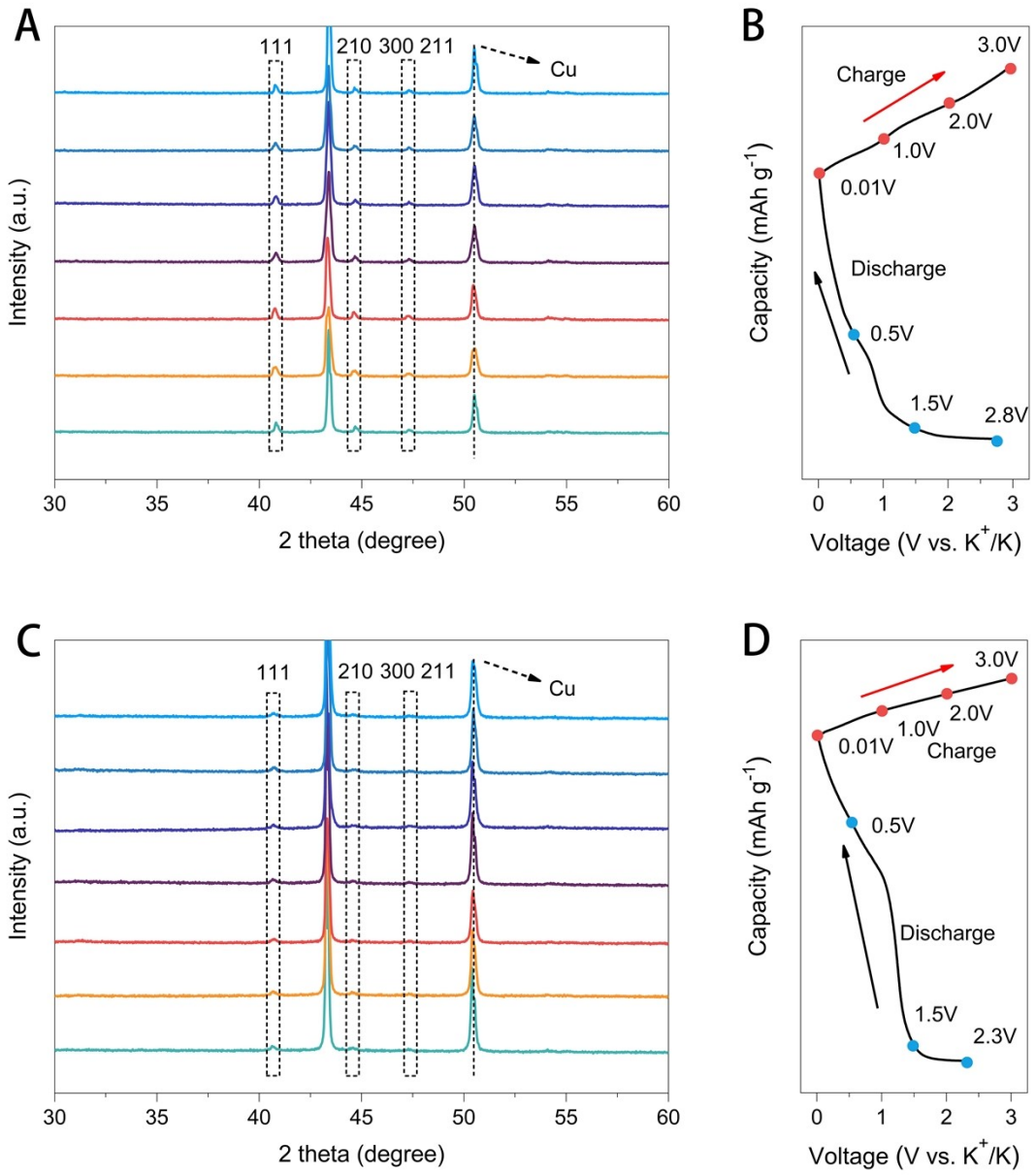

Figure S18. A) Ex situ XRD patterns of Ni_2P⊂N/P-CNS for LIBs and B) the corresponding charge–discharge curve of the first cycle. C) Ex situ XRD patterns of Ni_2P⊂N/P-CNS for SIBs and D) the corresponding charge–discharge curve of the first cycle.

Table S1. The elemental analysis results for the Ni_2P⊂N/P-CNS.

	C	N	H
Elemental content (%)	30.5	1.8	1.0

Table S2. Comparison of electrochemical performance of this work with previous materials applied in Potassium−ion batteries.

Materials	Current density (mA g^{-1}) /Capacity (mAh g^{-1})	Rate/Cycle number/Capacity decay rate (%)	Refs.
Ni_2P⊂N/P-CNS	1000/180	2000/0.016	This work
CNT/MoP	1000/252	1000/15.8	[S1]
CoP@NC	100/205.7	1200/13.2	[S2]
Ni-Fe-P/NC	500/172.9	1600/0.026	[S3]
Fe/C	50/288.9	50/36.8	[S4]
Cu_3P	1000/145.9	2000/6	[S5]
Ni_2P@GR	/	/	[S6]

Table S3. The fitting results for EIS of different materials.

	R_s (Ω)	R_{sf} (Ω)	R_{ct} (Ω)	R_p (Ω)
Ni_2P⊂N/P-CNS fresh	10.8	1001	1697	/
Ni_2P⊂N/P-CNS 10^{th} cycle	4.5	/	/	1568
Ni_2P⊂N/P-CNS 100^{th} cycle	3.7	/	/	929
Ni_2P	4.6	1885	>3000	
N/P-CNS	3.9	484.9	3086	

Note: R_s represents the resistance of the electrolyte. R_{ct} is assigned as the charge-transfer resistance. R_{sf} is the surface film resistance. R_p means all the impedance with the R_{ct} impedance decreased after several cycles.

Supplementary references:

[S1] Z. Wang, W. Gao, C. Ding, H. Qi, S. Kang and L. Cui, *J. Colloid Interface Sci.* **2021**, *584*, 875.

[S2] Y. Yun, B. Xi, F. Tian, W. Chen, W. Sun, H. Pan, J. Feng, Y. Qian and S. Xiong, *Adv. Energy Mater.* **2021**, *12*, 2103341.

[S3] X. Chen, S. Zeng, H. Muheiyati, Y. Zhai, C. Li, X. Ding, L. Wang, D. Wang, L. Xu, Y. He and Y. Qian, *ACS Energy Lett.* **2019**, *4*, 1496.

[S4] W. Li, B. Yan, H. Fan, C. Zhang, H. Xu, X. Cheng, Z. Li, G. Jia, S. An and X. Qiu, *ACS Appl. Mater. Interfaces* **2019**, *11*, 22364.

[S5] Y. Yun, B. Xi, Y. Gu, F. Tian, W. Chen, J. Feng, Y. Qian and S. Xiong, *J. Energy Chem.* **2022**, *66*, 339.

[S6] Y.-S. Kim, M.-C. Kim, S.-H. Moon, H. Kim and K.-W. Park, *Electroch. Acta* **2020**, *341*.